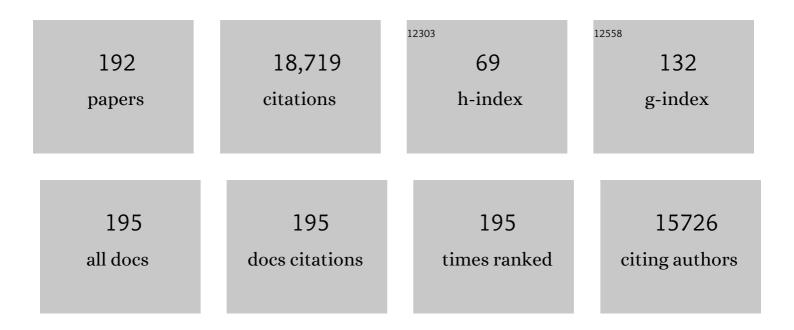
List of Publications by Year in descending order

Source: https://exaly.com/author-pdf/4730333/publications.pdf Version: 2024-02-01



YARING OL

#	Article	IF	CITATIONS
1	Recent Progress on Metal Halide Perovskite Solar Minimodules. Solar Rrl, 2022, 6, 2100458.	3.1	21
2	Atomic Level Insights into Metal Halide Perovskite Materials by Scanning Tunneling Microscopy and Spectroscopy. Angewandte Chemie - International Edition, 2022, 61, .	7.2	3
3	Atomic level insights intoÂmetal halide perovskiteÂmaterials by scanning tunneling microscopy and spectroscopy. Angewandte Chemie, 2022, 134, e202112352.	1.6	0
4	Synergistic stabilization of CsPbI3 inorganic perovskite via 1D capping and secondary growth. Journal of Energy Chemistry, 2022, 68, 387-392.	7.1	16
5	Investigating lithium metal anodes with nonaqueous electrolytes for safe and high-performance batteries. Sustainable Energy and Fuels, 2022, 6, 954-970.	2.5	11
6	Heterogeneous FASnI3 Absorber with Enhanced Electric Field for High-Performance Lead-Free Perovskite Solar Cells. Nano-Micro Letters, 2022, 14, 99.	14.4	43
7	From film to ring: Quasi-circular inorganic lead halide perovskite grain induced growth of uniform lead silicate glass ring structure. Applied Physics Letters, 2022, 120, .	1.5	1
8	Robust hole transport material with interface anchors enhances the efficiency and stability of inverted formamidinium–cesium perovskite solar cells with a certified efficiency of 22.3%. Energy and Environmental Science, 2022, 15, 2567-2580.	15.6	46
9	Perovskite solar cells by vapor deposition based and assisted methods. Applied Physics Reviews, 2022, 9, .	5.5	33
10	Understanding the nucleation and growth of the degenerated surface structure of the layered transition metal oxide cathodes for lithium-ion batteries by operando Raman spectroscopy. Journal of Electroanalytical Chemistry, 2022, 915, 116340.	1.9	1
11	Modulating crystal growth of formamidinium–caesium perovskites for over 200 cm2 photovoltaic sub-modules. Nature Energy, 2022, 7, 528-536.	19.8	89
12	Residual strain reduction leads to efficiency and operational stability improvements in flexible perovskite solar cells. Materials Advances, 2022, 3, 6316-6323.	2.6	10
13	Metal halide perovskite-based flexible tandem solar cells: next-generation flexible photovoltaic technology. Materials Chemistry Frontiers, 2021, 5, 4833-4850.	3.2	15
14	Scalable Fabrication of >90 cm ² Perovskite Solar Modules with >1000 h Operational Stability Based on the Intermediate Phase Strategy. Advanced Energy Materials, 2021, 11, 2003712.	10.2	76
15	Atomic-scale insight into the enhanced surface stability of methylammonium lead iodide perovskite by controlled deposition of lead chloride. Energy and Environmental Science, 2021, 14, 4541-4554.	15.6	31
16	Metal halide perovskite solar cells by modified chemical vapor deposition. Journal of Materials Chemistry A, 2021, 9, 22759-22780.	5.2	22
17	Two-Dimensional Dion–Jacobson Structure Perovskites for Efficient Sky-Blue Light-Emitting Diodes. ACS Energy Letters, 2021, 6, 908-914.	8.8	49
18	2D materials for conducting holes from grain boundaries in perovskite solar cells. Light: Science and Applications, 2021, 10, 68.	7.7	59

#	Article	IF	CITATIONS
19	Slot-die coating large-area formamidinium-cesium perovskite film for efficient and stable parallel solar module. Science Advances, 2021, 7, .	4.7	165
20	Lead halide–templated crystallization of methylamine-free perovskite for efficient photovoltaic modules. Science, 2021, 372, 1327-1332.	6.0	351
21	Unclonable Microâ€Texture with Clonable Microâ€Shape towards Rapid, Convenient, and Lowâ€Cost Fluorescent Antiâ€Counterfeiting Labels. Small, 2021, 17, e2100244.	5.2	28
22	Phase Aggregation Suppression of Homogeneous Perovskites Processed in Ambient Condition toward Efficient Lightâ€Emitting Diodes. Advanced Functional Materials, 2021, 31, 2103399.	7.8	18
23	Up-Scalable Fabrication of SnO2 with Multifunctional Interface for High Performance Perovskite Solar Modules. Nano-Micro Letters, 2021, 13, 155.	14.4	40
24	The Main Progress of Perovskite Solar Cells in 2020–2021. Nano-Micro Letters, 2021, 13, 152.	14.4	250
25	Atomic Scale Investigation of the CuPc–MAPbX ₃ Interface and the Effect of Non-Stoichiometric Perovskite Films on Interfacial Structures. ACS Nano, 2021, 15, 14813-14821.	7.3	8
26	Long-life lithium-sulfur batteries with high areal capacity based on coaxial CNTs@TiN-TiO2 sponge. Nature Communications, 2021, 12, 4738.	5.8	109
27	Narrow-Band Violet-Light-Emitting Diodes Based on Stable Cesium Lead Chloride Perovskite Nanocrystals. ACS Energy Letters, 2021, 6, 3545-3554.	8.8	39
28	Removal of residual compositions by powder engineering for high efficiency formamidinium-based perovskite solar cells with operation lifetime over 2000Ah. Nano Energy, 2021, 87, 106152.	8.2	41
29	Strategies and methods for fabricating high quality metal halide perovskite thin films for solar cells. Journal of Energy Chemistry, 2021, 60, 300-333.	7.1	31
30	Defect Passivation for Perovskite Solar Cells: from Molecule Design to Device Performance. ChemSusChem, 2021, 14, 4354-4376.	3.6	43
31	Recent progress on all-inorganic metal halide perovskite solar cells. Materials Today Nano, 2021, 16, 100143.	2.3	13
32	A solid–liquid hybrid electrolyte for lithium ion batteries enabled by a single-body polymer/indium tin oxide architecture. Journal Physics D: Applied Physics, 2021, 54, 475501.	1.3	3
33	CsPbBrxI3-x thin films with multiple ammonium ligands for low turn-on pure-red perovskite light-emitting diodes. Nano Research, 2021, 14, 191-197.	5.8	34
34	Spectral Stable Blue-Light-Emitting Diodes via Asymmetric Organic Diamine Based Dion–Jacobson Perovskites. Journal of the American Chemical Society, 2021, 143, 19711-19718.	6.6	29
35	Progress of Surface Science Studies on ABX ₃ â€Based Metal Halide Perovskite Solar Cells. Advanced Energy Materials, 2020, 10, 1902726.	10.2	87
36	Verringerung schÃ d licher Defekte für leistungsstarke Metallhalogenidâ€Perowskit‣olarzellen. Angewandte Chemie, 2020, 132, 6740-6764.	1.6	16

#	Article	IF	CITATIONS
37	Reducing Detrimental Defects for Highâ€Performance Metal Halide Perovskite Solar Cells. Angewandte Chemie - International Edition, 2020, 59, 6676-6698.	7.2	334
38	Recent Progress of Allâ€Bromide Inorganic Perovskite Solar Cells. Energy Technology, 2020, 8, 1900961.	1.8	66
39	Interface engineering strategies towards Cs ₂ AgBiBr ₆ single-crystalline photodetectors with good Ohmic contact behaviours. Journal of Materials Chemistry C, 2020, 8, 276-284.	2.7	78
40	Surface Termination-Dependent Nanotribological Properties of Single-Crystal MAPbBr ₃ Surfaces. Journal of Physical Chemistry C, 2020, 124, 1484-1491.	1.5	15
41	Efficient Anti-solvent-free Spin-Coated and Printed Sn-Perovskite Solar Cells with Crystal-Based Precursor Solutions. Matter, 2020, 2, 167-180.	5.0	38
42	Additives in metal halide perovskite films and their applications in solar cells. Journal of Energy Chemistry, 2020, 46, 215-228.	7.1	64
43	Increase the rigidity and hydrophobicity of perovskite by a molecular design. Science Bulletin, 2020, 65, 175-176.	4.3	3
44	Rapid hybrid chemical vapor deposition for efficient and hysteresis-free perovskite solar modules with an operation lifetime exceeding 800 hours. Journal of Materials Chemistry A, 2020, 8, 23404-23412.	5.2	34
45	A holistic approach to interface stabilization for efficient perovskite solar modules with over 2,000-hour operational stability. Nature Energy, 2020, 5, 596-604.	19.8	274
46	Photon Upconverting Solid Films with Improved Efficiency for Endowing Perovskite Solar Cells with Nearâ€Infrared Sensitivity. ChemPhotoChem, 2020, 4, 5271-5278.	1.5	26
47	In-situ passivation perovskite targeting efficient light-emitting diodes via spontaneously formed silica network. Nano Energy, 2020, 78, 105134.	8.2	28
48	The Impact of Atmosphere on Energetics of Lead Halide Perovskites. Advanced Energy Materials, 2020, 10, 2000908.	10.2	12
49	2D Derivative Phase Induced Growth of 3D All Inorganic Perovskite Micro–Nanowire Array Based Photodetectors. Advanced Functional Materials, 2020, 30, 2002526.	7.8	26
50	Inverse Growth of Large-Grain-Size and Stable Inorganic Perovskite Micronanowire Photodetectors. ACS Applied Materials & Interfaces, 2020, 12, 14185-14194.	4.0	30
51	Organic additive engineering toward efficient perovskite lightâ€emitting diodes. InformaÄnÃ-Materiály, 2020, 2, 1095-1108.	8.5	26
52	Imaging of the Atomic Structure of All-Inorganic Halide Perovskites. Journal of Physical Chemistry Letters, 2020, 11, 818-823.	2.1	26
53	How far are we from attaining 10-year lifetime for metal halide perovskite solar cells?. Materials Science and Engineering Reports, 2020, 140, 100545.	14.8	67
54	Highly Efficient Perovskite Solar Cells Enabled by Multiple Ligand Passivation. Advanced Energy Materials, 2020, 10, 1903696.	10.2	205

#	Article	IF	CITATIONS
55	Approaching isotropic transfer integrals in crystalline organic semiconductors. Physical Review Materials, 2020, 4, .	0.9	5
56	Thermodynamically stabilized β-CsPbI ₃ –based perovskite solar cells with efficiencies >18%. Science, 2019, 365, 591-595.	6.0	963
57	Phase transition induced recrystallization and low surface potential barrier leading to 10.91%-efficient CsPbBr3 perovskite solar cells. Nano Energy, 2019, 65, 104015.	8.2	170
58	Accelerating hole extraction by inserting 2D Ti ₃ C ₂ -MXene interlayer to all inorganic perovskite solar cells with long-term stability. Journal of Materials Chemistry A, 2019, 7, 20597-20603.	5.2	130
59	Atomic-scale view of stability and degradation of single-crystal MAPbBr ₃ surfaces. Journal of Materials Chemistry A, 2019, 7, 20760-20766.	5.2	46
60	Scalable Fabrication of Metal Halide Perovskite Solar Cells and Modules. ACS Energy Letters, 2019, 4, 2147-2167.	8.8	161
61	Carbon-Based Electrode Engineering Boosts the Efficiency of All Low-Temperature-Processed Perovskite Solar Cells. ACS Energy Letters, 2019, 4, 2032-2039.	8.8	79
62	Engineering Green-to-Blue Emitting CsPbBr ₃ Quantum-Dot Films with Efficient Ligand Passivation. ACS Energy Letters, 2019, 4, 2731-2738.	8.8	43
63	Surface Defect Dynamics in Organic–Inorganic Hybrid Perovskites: From Mechanism to Interfacial Properties. ACS Nano, 2019, 13, 12127-12136.	7.3	56
64	A redox shuttle imparts operational durability to perovskite solar cells. Science Bulletin, 2019, 64, 224-226.	4.3	4
65	Highly Efficient and Stable Perovskite Solar Cells via Modification of Energy Levels at the Perovskite/Carbon Electrode Interface. Advanced Materials, 2019, 31, e1804284.	11.1	161
66	Lithium-ion batteries: outlook on present, future, and hybridized technologies. Journal of Materials Chemistry A, 2019, 7, 2942-2964.	5.2	1,266
67	Reduction of lead leakage from damaged lead halide perovskite solar modules using self-healing polymer-based encapsulation. Nature Energy, 2019, 4, 585-593.	19.8	327
68	Progress of All-inorganic Cesium Lead-free Perovskite Solar Cells. Chemistry Letters, 2019, 48, 989-1005.	0.7	19
69	Improved SnO ₂ Electron Transport Layers Solutionâ€Deposited at Near Room Temperature for Rigid or Flexible Perovskite Solar Cells with High Efficiencies. Advanced Energy Materials, 2019, 9, 1900834.	10.2	100
70	Thermal degradation of formamidinium based lead halide perovskites into <i>sym</i> -triazine and hydrogen cyanide observed by coupled thermogravimetry-mass spectrometry analysis. Journal of Materials Chemistry A, 2019, 7, 16912-16919.	5.2	163
71	Determination of Carrier Diffusion Length Using Transient Electron Photoemission Microscopy in the GaAs/InSe Heterojunction. Physica Status Solidi (B): Basic Research, 2019, 256, 1900126.	0.7	1
72	Degradation Mechanism and Relative Stability of Methylammonium Halide Based Perovskites Analyzed on the Basis of Acid–Base Theory. ACS Applied Materials & Interfaces, 2019, 11, 12586-12593.	4.0	55

#	Article	IF	CITATIONS
73	High Efficient Hole Extraction and Stable Allâ€Bromide Inorganic Perovskite Solar Cells via Derivativeâ€Phase Gradient Bandgap Architecture. Solar Rrl, 2019, 3, 1900030.	3.1	67
74	Significant THz absorption in CH3NH2 molecular defect-incorporated organic-inorganic hybrid perovskite thin film. Scientific Reports, 2019, 9, 5811.	1.6	26
75	Elucidating the Mechanism Involved in the Performance Improvement of Lithiumâ€ion Transition Metal Oxide Battery by Conducting Polymer. Advanced Materials Interfaces, 2019, 6, 1801785.	1.9	18
76	Hybrid chemical vapor deposition enables scalable and stable Cs-FA mixed cation perovskite solar modules with a designated area of 91.8 cm ² approaching 10% efficiency. Journal of Materials Chemistry A, 2019, 7, 6920-6929.	5.2	112
77	Negligibleâ€Pbâ€Waste and Upscalable Perovskite Deposition Technology for Highâ€Operationalâ€Stability Perovskite Solar Modules. Advanced Energy Materials, 2019, 9, 1803047.	10.2	68
78	Influences of Spiro-MeOTAD Hole Transport Layer on the Long-term Stabilities of Perovskite-based Solar Cells. , 2019, , .		0
79	Perovskite Material and Solar Cell Research by Surface Science and Advanced Characterization. , 2019, , \cdot		0
80	Highly stable and efficient all-inorganic lead-free perovskite solar cells with native-oxide passivation. Nature Communications, 2019, 10, 16.	5.8	430
81	Unraveling the Impact of Halide Mixing on Perovskite Stability. Journal of the American Chemical Society, 2019, 141, 3515-3523.	6.6	116
82	Scalable Fabrication of Stable High Efficiency Perovskite Solar Cells and Modules Utilizing Room Temperature Sputtered SnO ₂ Electron Transport Layer. Advanced Functional Materials, 2019, 29, 1806779.	7.8	118
83	Stacked-graphene layers as engineered solid-electrolyte interphase (SEI) grown by chemical vapour deposition for lithium-ion batteries. Carbon, 2018, 132, 678-690.	5.4	16
84	Spin-Coated Crystalline Molecular Monolayers for Performance Enhancement in Organic Field-Effect Transistors. Journal of Physical Chemistry Letters, 2018, 9, 1318-1323.	2.1	37
85	Photodecomposition and thermal decomposition in methylammonium halide lead perovskites and inferred design principles to increase photovoltaic device stability. Journal of Materials Chemistry A, 2018, 6, 9604-9612.	5.2	437
86	Enhancing Optical, Electronic, Crystalline, and Morphological Properties of Cesium Lead Halide by Mn Substitution forÂHigh‧tability Allâ€ŀnorganic Perovskite Solar Cells withÂCarbon Electrodes. Advanced Energy Materials, 2018, 8, 1800504.	10.2	272
87	Research progress on organic–inorganic halide perovskite materials and solar cells. Journal Physics D: Applied Physics, 2018, 51, 093001.	1.3	56
88	Photovoltaics: Recent Advances in Spiroâ€MeOTAD Hole Transport Material and Its Applications in Organic–Inorganic Halide Perovskite Solar Cells (Adv. Mater. Interfaces 1/2018). Advanced Materials Interfaces, 2018, 5, 1870003.	1.9	3
89	Largeâ€Area Perovskite Solar Modules: Combination of Hybrid CVD and Cation Exchange for Upscaling Cs‧ubstituted Mixed Cation Perovskite Solar Cells with High Efficiency and Stability (Adv. Funct.) Tj ETQq1 1	0.7 ≿ €314 r	gBiT /Overloo
90	Scanning Probe Microscopy Applied to Organic–Inorganic Halide Perovskite Materials and Solar Cells. Small Methods, 2018, 2, 1700295.	4.6	57

#	Article	IF	CITATIONS
91	High-throughput surface preparation for flexible slot die coated perovskite solar cells. Organic Electronics, 2018, 54, 72-79.	1.4	24
92	Engineering Interface Structure to Improve Efficiency and Stability of Organometal Halide Perovskite Solar Cells. Journal of Physical Chemistry B, 2018, 122, 511-520.	1.2	68
93	Recent Advances in Spiroâ€MeOTAD Hole Transport Material and Its Applications in Organic–Inorganic Halide Perovskite Solar Cells. Advanced Materials Interfaces, 2018, 5, 1700623.	1.9	316
94	Scalable solution coating of the absorber for perovskite solar cells. Journal of Energy Chemistry, 2018, 27, 1101-1110.	7.1	44
95	Advances and challenges to the commercialization of organic–inorganic halide perovskite solar cell technology. Materials Today Energy, 2018, 7, 169-189.	2.5	231
96	Fully Solutionâ€Processed TCOâ€Free Semitransparent Perovskite Solar Cells for Tandem and Flexible Applications. Advanced Energy Materials, 2018, 8, 1701569.	10.2	77
97	Combination of Hybrid CVD and Cation Exchange for Upscaling Csâ€Substituted Mixed Cation Perovskite Solar Cells with High Efficiency and Stability. Advanced Functional Materials, 2018, 28, 1703835.	7.8	158
98	Themed issue on perovskite solar cells: research on metal halide perovskite solar cells towards deeper understanding, upscalable fabrication, long-term stability and Pb-free alternatives. Sustainable Energy and Fuels, 2018, 2, 2378-2380.	2.5	6
99	Gas-solid reaction based over one-micrometer thick stable perovskite films for efficient solar cells and modules. Nature Communications, 2018, 9, 3880.	5.8	109
100	Flexible and stable high-energy lithium-sulfur full batteries with only 100% oversized lithium. Nature Communications, 2018, 9, 4480.	5.8	193
101	Fabrication of efficient metal halide perovskite solar cells by vacuum thermal evaporation: A progress review. Current Opinion in Electrochemistry, 2018, 11, 130-140.	2.5	51
102	Progress toward Stable Lead Halide Perovskite Solar Cells. Joule, 2018, 2, 1961-1990.	11.7	181
103	Transition metal speciation as a degradation mechanism with the formation of a solid-electrolyte interphase (SEI) in Ni-rich transition metal oxide cathodes. Journal of Materials Chemistry A, 2018, 6, 14449-14463.	5.2	37
104	Energy Level Alignment at Interfaces in Metal Halide Perovskite Solar Cells. Advanced Materials Interfaces, 2018, 5, 1800260.	1.9	215
105	"Heat Wave―of Metal Halide Perovskite Solar Cells Continues in Phoenix. ACS Energy Letters, 2018, 3, 1898-1903.	8.8	5
106	Benchmarking Chemical Stability of Arbitrarily Mixed 3D Hybrid Halide Perovskites for Solar Cell Applications. Small Methods, 2018, 2, 1800242.	4.6	26
107	Interfacial Flat-Lying Molecular Monolayers for Performance Enhancement in Organic Field-Effect Transistors. ACS Applied Materials & Interfaces, 2018, 10, 22513-22519.	4.0	18
108	The influence of secondary solvents on the morphology of a spiro-MeOTAD hole transport layer for lead halide perovskite solar cells. Journal Physics D: Applied Physics, 2018, 51, 294001.	1.3	23

#	Article	IF	CITATIONS
109	Improved Efficiency and Stability of Perovskite Solar Cells Induced by CO Functionalized Hydrophobic Ammoniumâ€Based Additives. Advanced Materials, 2018, 30, 1703670.	11.1	132
110	Advances and Obstacles on Perovskite Solar Cell Research from Material Properties to Photovoltaic Function. ACS Energy Letters, 2017, 2, 520-523.	8.8	38
111	Transferrable optimization of spray-coated PbI ₂ films for perovskite solar cell fabrication. Journal of Materials Chemistry A, 2017, 5, 5709-5718.	5.2	54
112	Accelerated degradation of methylammonium lead iodide perovskites induced by exposure to iodine vapour. Nature Energy, 2017, 2, .	19.8	491
113	Application of Methylamine Gas in Fabricating Organic–Inorganic Hybrid Perovskite Solar Cells. Energy Technology, 2017, 5, 1750-1761.	1.8	46
114	Ultrahigh mobility and efficient charge injection in monolayer organic thin-film transistors on boron nitride. Science Advances, 2017, 3, e1701186.	4.7	146
115	Low ost Alternative Highâ€Performance Holeâ€Transport Material for Perovskite Solar Cells and Its Comparative Study with Conventional SPIROâ€OMeTAD. Advanced Electronic Materials, 2017, 3, 1700139.	2.6	60
116	Interfacial Modification of Perovskite Solar Cells Using an Ultrathin MAI Layer Leads to Enhanced Energy Level Alignment, Efficiencies, and Reproducibility. Journal of Physical Chemistry Letters, 2017, 8, 3947-3953.	2.1	101
117	Perovskite Solar Cells—Towards Commercialization. ACS Energy Letters, 2017, 2, 1749-1751.	8.8	107
118	Progress on Perovskite Materials and Solar Cells with Mixed Cations and Halide Anions. ACS Applied Materials & Interfaces, 2017, 9, 30197-30246.	4.0	453
119	Methylammonium Lead Bromide Perovskite Light-Emitting Diodes by Chemical Vapor Deposition. Journal of Physical Chemistry Letters, 2017, 8, 3193-3198.	2.1	113
120	Transamidation of dimethylformamide during alkylammonium lead triiodide film formation for perovskite solar cells. Journal of Materials Research, 2017, 32, 45-55.	1.2	37
121	Graphene specimen support technique for low voltage STEM imaging. Journal of Electron Microscopy, 2017, 66, 261-271.	0.9	3
122	Chemical vapor deposition grown formamidinium perovskite solar modules with high steady state power and thermal stability. Journal of Materials Chemistry A, 2016, 4, 13125-13132.	5.2	169
123	Moisture and Oxygen Enhance Conductivity of LiTFSIâ€Doped Spiroâ€MeOTAD Hole Transport Layer in Perovskite Solar Cells. Advanced Materials Interfaces, 2016, 3, 1600117.	1.9	123
124	The Effect of Impurities on the Impedance Spectroscopy Response of CH ₃ NH ₃ PbI ₃ Perovskite Solar Cells. Journal of Physical Chemistry C, 2016, 120, 28519-28526.	1.5	35
125	The presence of CH3NH2 neutral species in organometal halide perovskite films. Applied Physics Letters, 2016, 108, .	1.5	50
126	Measurement of high carrier mobility in graphene in an aqueous electrolyte environment. Applied Physics Letters, 2016, 109, .	1.5	37

#	Article	IF	CITATIONS
127	Post-annealing of MAPbI ₃ perovskite films with methylamine for efficient perovskite solar cells. Materials Horizons, 2016, 3, 548-555.	6.4	141
128	Role of the Dopants on the Morphological and Transport Properties of Spiro-MeOTAD Hole Transport Layer. Chemistry of Materials, 2016, 28, 5702-5709.	3.2	194
129	Thermal degradation of CH ₃ NH ₃ Pbl ₃ perovskite into NH ₃ and CH ₃ I gases observed by coupled thermogravimetry–mass spectrometry analysis. Energy and Environmental Science, 2016, 9, 3406-3410.	15.6	616
130	Surface and Interface Aspects of Organometal Halide Perovskite Materials and Solar Cells. Journal of Physical Chemistry Letters, 2016, 7, 4764-4794.	2.1	177
131	Dopant interdiffusion effects in n-i-p structured spiro-OMeTAD hole transport layer of organometal halide perovskite solar cells. Organic Electronics, 2016, 31, 71-76.	1.4	29
132	Universal energy level tailoring of self-organized hole extraction layers in organic solar cells and organic–inorganic hybrid perovskite solar cells. Energy and Environmental Science, 2016, 9, 932-939.	15.6	218
133	Rapid perovskite formation by CH ₃ NH ₂ gas-induced intercalation and reaction of PbI ₂ . Journal of Materials Chemistry A, 2016, 4, 2494-2500.	5.2	115
134	Properties and solar cell applications of Pb-free perovskite films formed by vapor deposition. RSC Advances, 2016, 6, 2819-2825.	1.7	131
135	Organometal halide perovskite thin films and solar cells by vapor deposition. Journal of Materials Chemistry A, 2016, 4, 6693-6713.	5.2	210
136	Perovskite Solar Cells: Silver Iodide Formation in Methyl Ammonium Lead Iodide Perovskite Solar Cells with Silver Top Electrodes (Adv. Mater. Interfaces 13/2015). Advanced Materials Interfaces, 2015, 2, .	1.9	7
137	Silver Iodide Formation in Methyl Ammonium Lead Iodide Perovskite Solar Cells with Silver Top Electrodes. Advanced Materials Interfaces, 2015, 2, 1500195.	1.9	646
138	Only the chemical state of Indium changes in Mn-doped In3Sb1Te2 (Mn: 10 at.%) during multi-level resistance changes. Scientific Reports, 2015, 4, 4702.	1.6	1
139	[Paper] p-Doping of Squaraine with F4-TCNQ by Solution Processing. ITE Transactions on Media Technology and Applications, 2015, 3, 133-142.	0.3	3
140	Pinhole-free hole transport layers significantly improve the stability of MAPbI ₃ -based perovskite solar cells under operating conditions. Journal of Materials Chemistry A, 2015, 3, 15451-15456.	5.2	122
141	Substantial improvement of perovskite solar cells stability by pinhole-free hole transport layer with doping engineering. Scientific Reports, 2015, 5, 9863.	1.6	119
142	Smooth perovskite thin films and efficient perovskite solar cells prepared by the hybrid deposition method. Journal of Materials Chemistry A, 2015, 3, 14631-14641.	5.2	126
143	Real-Space Imaging of the Atomic Structure of Organic–Inorganic Perovskite. Journal of the American Chemical Society, 2015, 137, 16049-16054.	6.6	155
144	Air-Exposure Induced Dopant Redistribution and Energy Level Shifts in Spin-Coated Spiro-MeOTAD Films. Chemistry of Materials, 2015, 27, 562-569.	3.2	357

#	Article	IF	CITATIONS
145	Influence of Air Annealing on High Efficiency Planar Structure Perovskite Solar Cells. Chemistry of Materials, 2015, 27, 1597-1603.	3.2	247
146	Large changes of graphene conductance as a function of lattice orientation between stacked layers. Nanotechnology, 2015, 26, 015702.	1.3	5
147	Flat-Lying Semiconductor–Insulator Interfacial Layer in DNTT Thin Films. ACS Applied Materials & Interfaces, 2015, 7, 1833-1840.	4.0	43
148	Mixed interlayers at the interface between PEDOT:PSS and conjugated polymers provide charge transport control. Journal of Materials Chemistry C, 2015, 3, 2664-2676.	2.7	26
149	Large formamidinium lead trihalide perovskite solar cells using chemical vapor deposition with high reproducibility and tunable chlorine concentrations. Journal of Materials Chemistry A, 2015, 3, 16097-16103.	5.2	165
150	Ultrathin polycrystalline 6,13-Bis(triisopropylsilylethynyl)-pentacene films. Journal of Vacuum Science and Technology A: Vacuum, Surfaces and Films, 2015, 33, 021506.	0.9	0
151	Temperature-dependent hysteresis effects in perovskite-based solar cells. Journal of Materials Chemistry A, 2015, 3, 9074-9080.	5.2	121
152	Air-Exposure-Induced Gas-Molecule Incorporation into Spiro-MeOTAD Films. Journal of Physical Chemistry Letters, 2014, 5, 1374-1379.	2.1	96
153	High performance perovskite solar cells by hybrid chemical vapor deposition. Journal of Materials Chemistry A, 2014, 2, 18742-18745.	5.2	284
154	Reliability improvement of bulk-heterojunction organic solar cell by using reduced graphene oxide as hole-transport layer. Physica Status Solidi (A) Applications and Materials Science, 2014, 211, 1873-1876.	0.8	5
155	Fabrication of semi-transparent perovskite films with centimeter-scale superior uniformity by the hybrid deposition method. Energy and Environmental Science, 2014, 7, 3989-3993.	15.6	213
156	Observation of chemical separation of In3Sb1Te2 thin film during phase transition. Applied Surface Science, 2014, 292, 986-989.	3.1	6
157	Electrical and optical properties of transparent flexible electrodes: Effects of UV ozone and oxygen plasma treatments. Organic Electronics, 2014, 15, 721-728.	1.4	23
158	Sensitivity to Molecular Order of the Electrical Conductivity in Oligothiophene Monolayer Films. Langmuir, 2013, 29, 1206-1210.	1.6	5
159	Charge transport across metal/molecular (alkyl) monolayer-Si junctions is dominated by the LUMO level. Physical Review B, 2012, 85, .	1.1	51
160	Solution doping of organic semiconductors using air-stable n-dopants. Applied Physics Letters, 2012, 100, .	1.5	86
161	Hybrid Heterocycle-Containing Electron-Transport Materials Synthesized by Regioselective Suzuki Cross-Coupling Reactions for Highly Efficient Phosphorescent OLEDs with Unprecedented Low Operating Voltage. Chemistry of Materials, 2012, 24, 3817-3827.	3.2	45
162	nâ€Đoping of Organic Electronic Materials using Air‣table Organometallics. Advanced Materials, 2012, 24, 699-703.	11.1	163

#	Article	IF	CITATIONS
163	Electrical Transport Properties of Oligothiophene-Based Molecular Films Studied by Current Sensing Atomic Force Microscopy. Nano Letters, 2011, 11, 4107-4112.	4.5	34
164	Soluble fullerene derivatives: The effect of electronic structure on transistor performance and air stability. Journal of Applied Physics, 2011, 110, .	1.1	19
165	Scanning Tunneling Microscopy in Surface Science, Nanoscience and Catalysis, Michael Bowker and Philip R. Davies (Eds.). Wiley-VCH, Weinheim, 2010, 244 pages. Print ISBN 9783527319824; Online ISBN 9783527628827. Microscopy and Microanalysis, 2011, 17, 132-132.	0.2	0
166	Investigation of organic films by atomic force microscopy: Structural, nanotribological and electrical properties. Surface Science Reports, 2011, 66, 379-393.	3.8	23
167	Filled and empty states of alkanethiol monolayer on Au (111): Fermi level asymmetry and implications for electron transport. Chemical Physics Letters, 2011, 511, 344-347.	1.2	46
168	Hexaazatriphenylene (HAT) versus triâ€HAT: The Bigger the Better?. Chemistry - A European Journal, 2011, 17, 10312-10322.	1.7	40
169	Electronic structure and band alignment of 9,10-phenanthrenequinone passivated silicon surfaces. Surface Science, 2011, 605, 1308-1312.	0.8	16
170	Ultra-flat coplanar electrodes for controlled electrical contact of molecular films. Review of Scientific Instruments, 2011, 82, 123901.	0.6	7
171	Silicon surface passivation by an organic overlayer of 9,10-phenanthrenequinone. Applied Physics Letters, 2010, 96, 222109.	1.5	40
172	The Influence of Film Morphology in Highâ€Mobility Smallâ€Molecule:Polymer Blend Organic Transistors. Advanced Functional Materials, 2010, 20, 2330-2337.	7.8	120
173	Modification of gold source and drain electrodes by self-assembled monolayer in staggered n- and p-channel organic thin film transistors. Organic Electronics, 2010, 11, 227-237.	1.4	108
174	Relative permittivity and Hubbard U of pentacene extracted from scanning tunneling microscopy studies of p-doped films. Chemical Physics Letters, 2010, 495, 212-217.	1.2	10
175	Probing nanotribological and electrical properties of organic molecular films with atomic force microscopy. Scanning, 2010, 32, 257-264.	0.7	10
176	Remote doping of a pentacene transistor: Control of charge transfer by molecular-level engineering. Applied Physics Letters, 2010, 97, .	1.5	36
177	A Molybdenum Dithiolene Complex as <i>p</i> -Dopant for Hole-Transport Materials: A Multitechnique Experimental and Theoretical Investigation. Chemistry of Materials, 2010, 22, 524-531.	3.2	65
178	Influence of Molecular Ordering on Electrical and Friction Properties of ï‰-(<i>trans</i> -4-Stilbene)Alkylthiol Self-Assembled Monolayers on Au (111). Langmuir, 2010, 26, 16522-16528.	1.6	19
179	Electrical transport and mechanical properties of alkylsilane self-assembled monolayers on silicon surfaces probed by atomic force microscopy. Journal of Chemical Physics, 2009, 130, 114705.	1.2	25
180	Use of a High Electron-Affinity Molybdenum Dithiolene Complex to p-Dope Hole-Transport Layers. Journal of the American Chemical Society, 2009, 131, 12530-12531.	6.6	91

#	Article	IF	CITATIONS
181	Surface Species Formed by the Adsorption and Dissociation of Water Molecules on a Ru(0001) Surface Containing a Small Coverage of Carbon Atoms Studied by Scanning Tunneling Microscopy. Journal of Physical Chemistry C, 2008, 112, 7445-7454.	1.5	50
182	Mechanical and Charge Transport Properties of Alkanethiol Self-Assembled Monolayers on a Au(111) Surface:  The Role of Molecular Tilt. Langmuir, 2008, 24, 2219-2223.	1.6	62
183	Noncontact to contact tunneling microscopy in self-assembled monolayers of alkylthiols on gold. Journal of Chemical Physics, 2008, 128, 234701.	1.2	8
184	Electronic contribution to friction on GaAs: An atomic force microscope study. Physical Review B, 2008, 77, .	1.1	75
185	Influence of carrier density on the friction properties of silicon <mml:math xmlns:mml="http://www.w3.org/1998/Math/MathML" display="inline"><mml:mrow><mml:mi>p</mml:mi>n</mml:mrow>junctions. Physical Review B. 2007. 76</mml:math 	1.1	50
186	Frequency-controlled interaction between magnetic microspheres. Applied Physics Letters, 2006, 88, 134107.	1.5	4
187	Band gaps from ring resonators and structural periodicity. Journal Physics D: Applied Physics, 2005, 38, 590-595.	1.3	5
188	Anisotropy properties of magnetic colloidal materials. Journal Physics D: Applied Physics, 2003, 36, L10-L14.	1.3	14
189	Influences of geometry of particles on electrorheological fluids. Journal Physics D: Applied Physics, 2002, 35, 2231-2235.	1.3	32
190	Effect of zinc doping on the microstructure in YBCO. Physica C: Superconductivity and Its Applications, 2000, 341-348, 669-670.	0.6	6
191	Perovskite Material and Solar Cell Research by Surface Science and Advanced Characterization. , 0, , .		0
192	Up-Scaling of Organic-Inorganic Hybrid Perovskite Solar Cells and Modules. , 0, , .		0